

Membrane Proteins

Specific Ion–Protein Interactions Influence Bacterial Ice Nucleation

Ralph Schwidetzky^{+, * [a]}, Max Lukas^{+, [a]}, Azade YazdanYar^{+, [a]}, Anna T. Kunert^{, [b]}, Ulrich Pöschl^{, [b]}, Katrin F. Domke^{, [a]}, Janine Fröhlich-Nowoisky^{, [b]}, Mischa Bonn^{, [a]}, Thomas Koop^{, [c]}, Yuki Nagata^{, [a]} and Konrad Meister^{*, [a, d]}

Abstract: Ice nucleation-active bacteria are the most efficient ice nucleators known, enabling the crystallization of water at temperatures close to 0 °C, thereby overcoming the kinetically hindered phase transition process at these conditions. Using highly specialized ice-nucleating proteins (INPs), they can cause frost damage to plants and influence the formation of clouds and precipitation in the atmosphere. In nature, the bacteria are usually found in aqueous environments containing ions. The impact of ions on bacterial ice nucleation efficiency, however, has remained elusive. Here, we demonstrate that ions can profoundly influence the efficiency of bacterial ice nucleators in a manner that follows

the Hofmeister series. Weakly hydrated ions inhibit bacterial ice nucleation whereas strongly hydrated ions apparently facilitate ice nucleation. Surface-specific sum-frequency generation spectroscopy and molecular dynamics simulations reveal that the different effects are due to specific interactions of the ions with the INPs on the surface of the bacteria. Our results demonstrate that heterogeneous ice nucleation facilitated by bacteria strongly depends upon the nature of the ions, and specific ion–protein interactions are essential for the complete description of heterogeneous ice nucleation by bacteria.

Introduction

At ambient conditions, the formation of ice from water is thermodynamically favored at temperatures below 0 °C, however, this crystallization process is kinetically hindered. As a result, pure water can be supercooled to temperatures as low as –38 °C, below which homogenous ice nucleation occurs.^[1] In natural systems, water freezes in a heterogeneous process, facilitated by the presence of ice-nucleating substances of biological and abiotic origins.^[2] Ice nucleation-active bacteria from *Pseudomonas syringae* are the best ice nucleators (IN) known,

and their ability to induce ice formation at high sub-zero temperatures has direct impacts on agriculture, microbial ecology, geology and precipitation patterns.^[3] The ability to nucleate ice is attributed to ice-nucleating proteins (INPs). INPs are monomeric but have repeatedly been shown to form functional aggregates in the bacterial outer membranes, and the largest INP aggregates (> 50 INPs) are thought to be responsible for enabling freezing close to 0 °C.^[4] INP-induced ice nucleation usually takes place in ionic solutions, because ions are omnipresent in the environment. Therefore, the effect of salts on the INP-mediated freezing of water is of fundamental interest. For homogenous ice nucleation, it is established that ice formation depends on the water activity of the given aqueous solution, independently of the nature of the present ions.^[1] In contrast, the effect of ions on heterogeneous ice formation facilitated by bacteria has remained largely elusive.^[3b, 5]

The interaction of ions with proteins can be categorized by the Hofmeister series and has been observed for numerous processes.^[6] In the 1880s, Franz Hofmeister ranked ions based on their ability to precipitate proteins from solution.^[7] The work resulted in the following rankings for anions: $\text{SO}_4^{2-} > \text{HPO}_4^{2-} > \text{CH}_3\text{COO}^- > \text{Cl}^- > \text{Br}^- > \text{I}^- > \text{SCN}^-$ and for cations: $[\text{C}(\text{NH}_2)_3]^+ (\text{Gdm}^+) > \text{Mg}^{2+} > \text{Ca}^{2+} > \text{Li}^+ > \text{Na}^+ > \text{NH}_4^+ > \text{N}(\text{CH}_3)_4^+$, respectively.^[8] Ions on the left side of the series stabilize and salt out proteins, whereas ions on the right denature and solubilize proteins. It is generally accepted that the Hofmeister series is an interfacial phenomenon, in which direct protein-ion-water interactions are of central significance.^[6a, 9] Here, we investigate the effects of different ions on the ice nu-


[a] R. Schwidetzky,⁺ M. Lukas,⁺ Dr. A. YazdanYar,⁺ Dr. K. F. Domke, Prof. Dr. M. Bonn, Dr. Y. Nagata, Prof. Dr. K. Meister
 Max Planck Institute for Polymer Research, 55128 Mainz (Germany)
 E-mail: schwidetzkyr@mpip-mainz.mpg.de
 meisterk@mpip-mainz.mpg.de


[b] Dr. A. T. Kunert, Prof. Dr. U. Pöschl, Dr. J. Fröhlich-Nowoisky
 Max Planck Institute for Chemistry, 55128 Mainz (Germany)

[c] Prof. Dr. T. Koop
 Bielefeld University, 33615 Bielefeld (Germany)

[d] Prof. Dr. K. Meister
 University of Alaska Southeast, 99801 Juneau, AK (USA)

[†] These authors contributed equally to this work.

 Supporting Information and the ORCID identification number(s) for the author(s) of this article can be found under:
<https://doi.org/10.1002/chem.202004630>.

 © 2021 The Authors. Chemistry - A European Journal published by Wiley-VCH GmbH. This is an open access article under the terms of the Creative Commons Attribution Non-Commercial NoDerivs License, which permits use and distribution in any medium, provided the original work is properly cited, the use is non-commercial and no modifications or adaptations are made.

cleation activity of the proteinaceous IN from *Pseudomonas syringae* (*P. syringae*).^[10]

Results and Discussion

Figure 1A shows the results of freezing experiments of a dilution series of the bacterial IN (Snomax) in water and in aqueous solutions containing either 0.5 mol kg⁻¹ NaCl, NH₄Cl, NaSCN or MgSO₄. The freezing spectra of the bacterial IN in water and in the presence of MgSO₄ look similar and show two increases in the cumulative number of IN per unit mass of bacteria, $N_m(T)$, at -2.9 °C and -7.5 °C with plateaus between -4.5 °C and -7 °C and below -9.5 °C. The two increases reveal that the ice nucleation activity of *P. syringae* is caused by two classes of IN with different activation temperatures, and we attribute them to class A and C IN, respectively.^[11] Class C IN is usually attributed to individual INPs or small assemblies in the bacterial membrane, and class A IN is thought to originate from larger clusters of class C IN, as shown in Figure 1B.

In the presence of NaCl, the freezing spectrum is identical to the one of *P. syringae* in pure water, with a ~2 °C shift of the INP-mediated freezing curve to lower temperatures. This observed shift is in line with the expected shift of -1.86 °C based on the colligative melting point depression properties of a 0.5 mol kg⁻¹ NaCl solution (see Supporting Information, Figure S1).^[12] For NH₄Cl and NaSCN solutions, the trends are markedly different from those of *P. syringae* in pure water or NaCl solution. In the presence of NH₄Cl, the class A-related increase at about -2.9 °C is absent; instead, we observe a small increase at -7 °C. Further, the second increase is observed at -9 °C, which again is ~2 °C lower than that in water and which is similar to the shift observed on adding NaCl. For NaSCN, we observe only a single increase centered at -11.5 °C. Evidently,

the four salts influence the efficiency of the INP-mediated freezing points differently.

We examined whether different water activities in the investigated salt solutions may be the origin of the observed ion-specific effects on bacterial ice nucleation. Accounting for the effects of water activity, we found that they do not alter the respective observed influence of the salts on the INP-mediated freezing point (Figure S2). In fact, NaCl, NH₄Cl, and NaSCN all have nearly identical water activities at 0.5 mol kg⁻¹. Yet, they differ significantly in their effect on the bacterial ice nucleation activity. Clearly, the effect of salts on heterogeneous ice nucleation facilitated by bacterial INPs is not simply determined by water activity, as holds for homogeneous nucleation, and requires further investigations.

We conducted a comprehensive experimental evaluation of seventeen salts of the Hofmeister series to obtain more details of the specific effects of ions on the bacterial activities of the INPs. The experimentally determined freezing points in the salt solutions shown in Figure 2 were corrected for their respective water activity by taking the shifted melting points into account (see Supporting Information).

Four major categories can be identified from the plotted salt induced shifts in freezing temperatures: (i) NaSCN influences both bacterial IN classes A and C and lowers their respective freezing temperatures; (ii) NH₄Cl lowers the freezing temperature of class A, but does not affect class C; (iii) NaCl has negligible effects on both freezing temperatures; and (iv) MgSO₄ increases the freezing temperatures of classes A and C. Interestingly, the effects of the salts on the INP-mediated freezing temperatures follows the individual position of the anions in the Hofmeister series. Weakly hydrated ions such as SCN⁻ lower the INP-mediated freezing temperatures, whereas salts that have no effects, or apparently facilitate freezing, are more strongly hydrated ions such as Cl⁻ or SO₄²⁻.

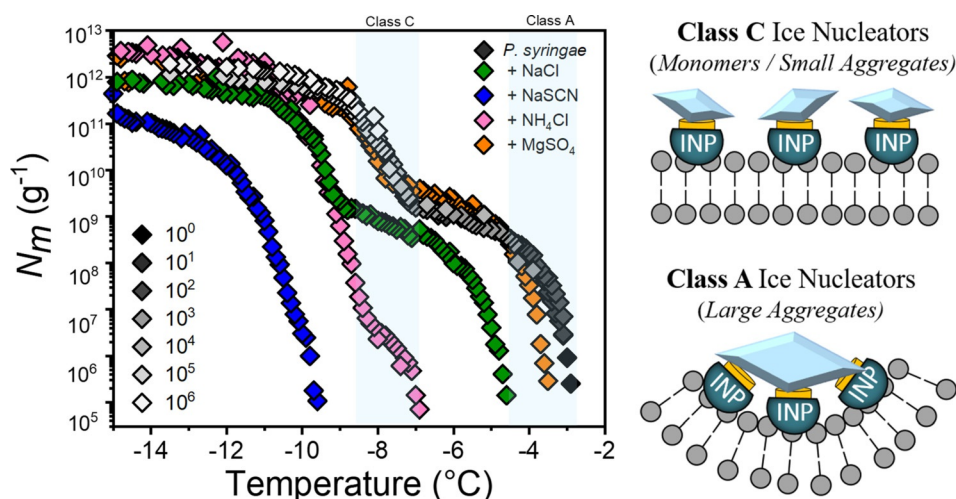


Figure 1. Freezing experiments of bacterial ice nucleators from *P. syringae* in aqueous solutions: (A) Results for IN in pure water (grey) and in aqueous solutions of 0.5 mol kg⁻¹ NaCl (green), NH₄Cl (magenta), NaSCN (blue), and MgSO₄ (orange). Plotted is the cumulative number of IN per unit mass of *P. syringae* vs. temperature for various degrees of dilution, starting with 0.1 mg mL⁻¹. Numbers and grey shades in the legend denote dilution factors and are shown for *P. syringae* in pure water only. The temperature ranges for class A and C bacterial IN in water are shaded in blue. (B) Proposed schematic illustration of class C and A IN structures. The high activity of bacterial IN relies on INPs, which assemble into larger functional protein clusters. The most effective IN clusters are termed class A, consisting of large INP assemblies. Class C IN are less active and consist of smaller INP assemblies.

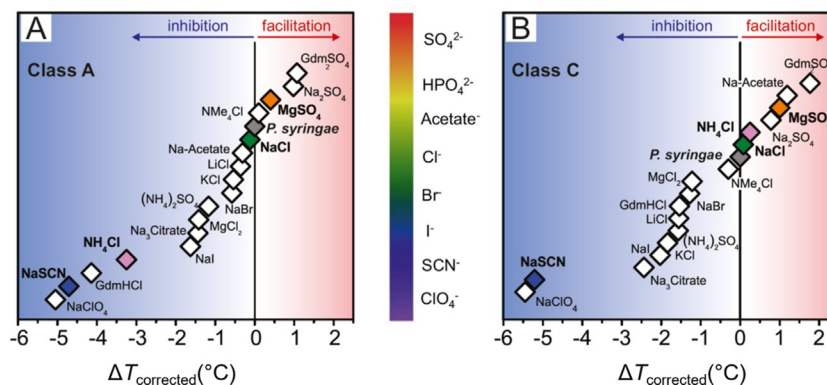


Figure 2. Effects of salts on the activity of bacterial IN from *P. syringae*: Shown are the temperature shifts (ΔT) induced by different salts on the freezing temperatures of class A and class C IN in water (grey diamonds). Vertically, the salts are ordered by the appearance of their anions in the Hofmeister series. The shifts represent the temperature difference for a frozen fraction of 50% of investigated samples ($f_{ice}=0.5$) between *P. syringae* in water and in the respective 0.5 mol kg^{-1} salt solution, the latter corrected for their water-activity effect (see Supporting Information). The concentration of *P. syringae* was 0.1 mg mL^{-1} for class A IN (A) and $10^{-6} \text{ mg mL}^{-1}$ for class C IN (B). The corresponding anion Hofmeister series is shown in the inset.

How can the different effects of the ions on the ice nucleation properties of the bacteria be explained? Different ions affect the local water structure, having different hydrogen-bond-forming and -breaking capabilities.^[6a] Ions can, however, also alter protein conformations, and we surmise that both effects could alter the freezing behavior of INPs.^[6a] Clearly, molecular-level information is required to explore both possibilities. The combination of sum-frequency generation (SFG) vibrational spectroscopy experiments and molecular dynamics (MD) simulations is ideally suited for elucidating biomolecular conformations and biomolecule-water interactions.^[4c,9b,13]

SFG is a surface-specific method in which an infrared and a visible pulse are combined at a surface to generate light at the sum-frequency of the two incident fields. The selection rule of this spectroscopy dictates that only ensembles of molecules with a net orientation, for example, at an interface, can generate a detectable signal. The SFG signal intensity depends on

the number of aligned molecules at the interface. Changes in the solution pH was shown to strongly affect the SFG spectral response of bacterial ice nucleators. Therefore, all SFG experiments were performed in PBS buffer since the addition of salts can affect the solution pH in an ion-specific manner.^[14] At charged surfaces, the surface field can align the water dipoles, as illustrated in Figure 3A. Such charge-induced enhanced ordering of the interfacial water molecules causes the SFG signal intensity in the O–H stretching region (IR wavenumber $\sim 3100\text{--}3600 \text{ cm}^{-1}$) to increase, and inversely, the SFG signal intensity can be used to quantify the amount of charge at the electrified surface. This concept has been used previously to investigate the effect of ions on biomolecules.^[6b,9b,14,15]

Figure 3B shows the SFG spectra of aqueous solutions of *P. syringae* adsorbed to the air–liquid interface in PBS buffer and in the presence of salts. The signals in the frequency region from $2800\text{--}3100 \text{ cm}^{-1}$ originate from C–H stretching vi-

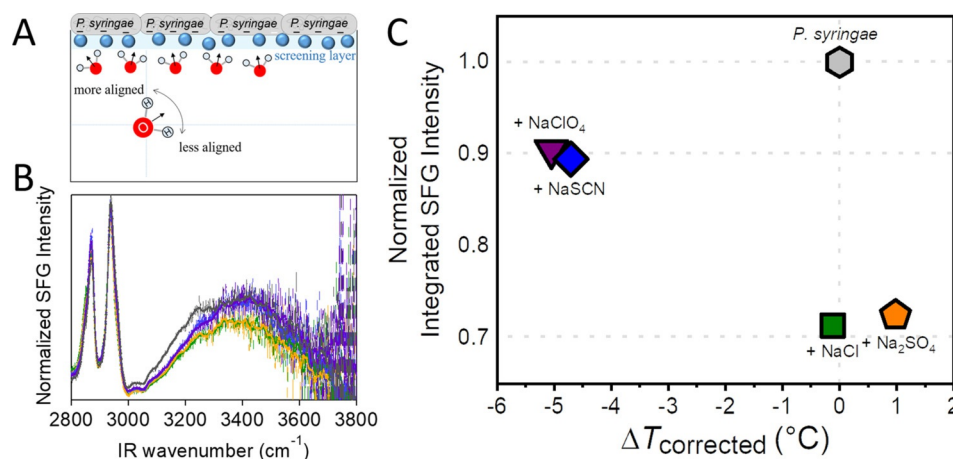


Figure 3. Sum-frequency generation spectroscopy measurements of bacterial ice nucleators from *P. syringae* in aqueous salt solutions: (A) Schematic representation of the orientation of interfacial water molecules next to *P. syringae* (grey) possessing a negative net charge. The straight arrows indicate the direction of the water dipoles and the blue spheres depict ions. The curved arrow indicates possible disruptions of the alignment due to the presence of salts. (B) SFG spectra of *P. syringae* layers at the air–liquid interface of a phosphate-buffered saline (PBS) solution (grey) and in the presence of NaCl (green), NaSCN (blue), NaClO₄ (purple) and Na₂SO₄ (orange). The bulk concentration of *P. syringae* was 0.1 mg mL^{-1} , and the salt concentrations were chosen to have identical ionic strength. (C) Normalized integrated SFG intensities of the frequency region from $3100\text{--}3600 \text{ cm}^{-1}$ for *P. syringae* in PBS and in the presence of salts plotted against the respective class A temperature shifts observed in the freezing experiments (Figure 2A).

brations. The broad signal between 3100–3600 cm^{-1} is assigned to the O–H stretching band of interfacial water molecules. We integrated the SFG signal in the frequency region of 3100–3600 cm^{-1} to allow for a direct quantitative comparison of the effects of the salts as shown in Figure 3C. The SFG intensity is highest in PBS buffer and decreases upon the addition of salts. This observation can be explained as follows: The cations of the salts screen the net negative charge of *P. syringae*, which in turn reduces the water molecules' alignment and causes the O–H stretch signal to decrease.^[15] Interestingly, the salts show different efficiencies in screening the net charge despite having identical ionic strengths. The weakly hydrated anions decrease the SFG intensity less than strongly hydrated anions like SO_4^{2-} . One explanation for this observation is the preferred adsorption of weakly hydrated anions to the *P. syringae* surface, rendering it more negative and, in turn, causing more water alignment and increasing the O–H signal intensity compared to strongly hydrated anions, which prefer to stay solvated (Scenario 1). A second explanation is that the ions can change the INP conformation, thereby affecting the charge distribution of the protein, which would alter the water alignment and thus the SFG signal (Scenario 2).

To distinguish between both scenarios, we performed MD simulations of the solvated INP in the presence of ions. The INP structure consists of fourteen repetitions of the amino acid sequence GYGSTQTSGSESSLTA as shown in Figure 4A. The INP model adapts a β -helical structure, in excellent agreement with

our circular dichroism spectrum of the purified INP (Figure S3). We particularly focused on the water orientation and ionic distribution near the proposed active sites of the INP^[16] and considered simulation settings, in which we kept the INP structure either flexible or fixed (see Experimental Section).

We analyzed the water orientation ($\langle \cos \theta \rangle$) relative to the IN planes of the INP in the presence of the different salts (Figure S4), where θ is the angle between the water molecule's bisector and the plane normal of the active sites (see Experimental Section). We can directly compare the experimental and computational findings by obtaining the square of the integrated $\rho \langle \cos \theta \rangle$ (ρ is the density of water), which is approximately proportional to the SFG intensity.^[17]

The comparison of the SFG intensities and the square of $\rho \langle \cos \theta \rangle$ (calculated SFG intensities) for the INP samples, presented in Figure 4B, reveals that the simulations reproduce the experimental trend and capture the effects of the different ions on the water orientation near the INP well. In agreement with the experiments, we observe that weakly hydrated ions are found near the INP surface, rendering the protein more negative and enhancing water orientation relative to the active IN planes, while strongly hydrated ions show a gradual increase in the population when moving away from the INP surface to the bulk water (Figure 4C). This finding is in line with Scenario 1 and consistent with the Hofmeister series. The depth profiles of the different ion species along the surface normal of the IN planes are further largely different (Fig-

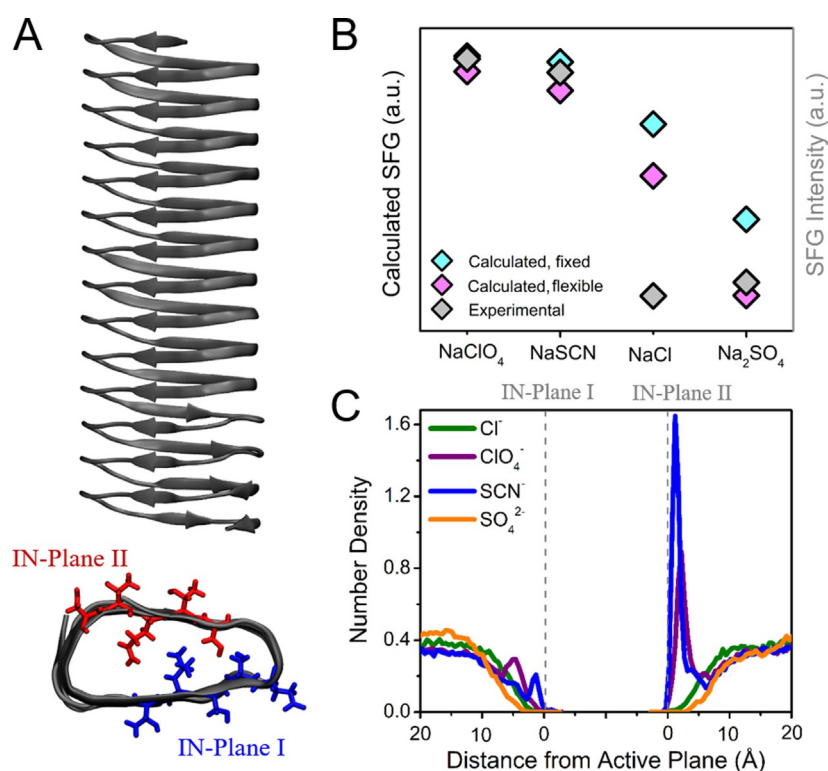


Figure 4. Molecular dynamics simulations of the INP from *P. syringae*: (A) Model of the INP from *P. syringae*, consisting of 14 repeats and forming a β -helical structure. The two ice-nucleating planes are highlighted in red and blue, respectively. (B) Calculated and experimental SFG intensities in the presence of four different salts. In the simulations, the INP structure was kept in either a fixed (cyan) or a flexible (magenta) geometry. (C) Distribution of the anions with respect to the two active ice-nucleating planes for the flexible geometry of the INP.

ure 4C), underlining the different ion interactions with the protein.

To elucidate the possible effect of the protein conformation on the water orientation and ion distributions (Scenario 2), we computed the water orientation near the INP by fixing the protein geometry in the MD simulation (see Experimental Section). The fixed structure of the INP shows the same trend for the ions, but the extent of the effects on the water orientation is reduced (Figure 4B). We also examined the depth profile of the ion distributions for the fixed geometry (Figure S5), and, compared to the flexible geometry, the weakly hydrated anions approach the fixed INP much less. Coming back to the two scenarios, these observations manifest, that the change of the INP conformation and the propensity of the ions affect the water ordering property as competing scenarios.

Conclusions

The above investigations suggest that ions affect the conformation and aggregation behavior of biomolecules in aqueous solutions very specifically, in addition to nonspecific electrostatic interactions. Our study provides unique insights into how different ions influence protein stability, aggregation, and, ultimately, the biological function of an organism. We provide clear evidence that the effect of ions on bacterial ice nucleation is not independent of the nature of the ion but is due to specific ion–protein interactions that follow the trend of the Hofmeister series.

Weakly hydrated anions like perchlorate can directly interact with individual INP units and change their conformations and disable their individual IN sites (Figure 4, Figure S3). The change in INP conformation further leads to the loss of the formation of the functional aggregates and collective alignment of INP units that enable freezing at -2°C (Figure 1). We also note that ion addition can affect the pH value of the aqueous solutions in an ion-specific manner. Such pH changes strongly influence the ice nucleation activity of *P. syringae* as shown before,^[3b,14] and those results are consistent with the observations made for NH_4Cl in this work. Hence, the observed ion-specific inhibitory effect of NH_4Cl is entirely due to the change of the solution pH (Figure S6).

Strongly hydrated ions enhance bacterial ice nucleation slightly. Sulfate ions were reported to decrease the reorientation time of water at the ice-binding site of antifreeze proteins^[18] and can create low-mobility water regions next to the active IN sites of the INP (see Experimental Section, Figures S7, S8). We speculate that such low-mobility regions may facilitate ice nucleation, in line with a recent MD simulation showing that low-mobility regions are the origin of seeds in homogeneous ice nucleation.^[19]

Undoubtedly, fully intact ice-nucleating protein (INP) structures and a precise sub-Ångström arrangement of INPs and water molecules are required for the extraordinary ice nucleation ability of INPs. The large variety of the salts investigated here, together with the different types of mechanisms by which ions affect bacterial IN, suggest that the general water activity-based ice nucleation criterion is not sufficient for a de-

tailed description of the effects of solutes on bacterial IN. The water-activity approach is valid for those cases, where the solutes do not directly affect the surfaces of ice nucleators, which is clearly not the case for the bacterial INPs studied here. We note that several of the salts studied here have direct biological and atmospheric relevance and are found at similar concentrations in the environment, for example, in natural cloud condensation nuclei.^[5a,20] As bacterial ice nucleation efficiency is controlled by complex and mutually interacting environmental variables such as the presence of co-solutes or pH value, these all must be taken into account for a complete understanding and a validated environmental application of bacterial ice nucleators' properties.

Acknowledgements

This work was financially supported by the MaxWater initiative of the Max Planck Society and the Max Planck Graduate Center with the Johannes Gutenberg-Universität Mainz. We thank Arpa Hudait and Valeria Molinero for providing the reconstructed INP structure file. A.Y.Y. and K.F.D. gratefully acknowledge funding through the "Plus 3" program of the Boehringer Ingelheim Stiftung. Open access funding enabled and organized by Projekt DEAL.

Conflict of interest

The authors declare no conflict of interest.

Keywords: atmospheric chemistry · bacteria · ice nucleation · Hofmeister series · nonlinear optics

- [1] T. Koop, B. P. Luo, A. Tsias, T. Peter, *Nature* **2000**, *406*, 611–614.
- [2] a) P. W. Wilson, A. F. Heneghan, A. D. Haymet, *Cryobiology* **2003**, *46*, 88–98; b) L. R. Maki, K. J. Willoughby, *J. Appl. Meteorol.* **1978**, *17*, 1049–1053; c) K. Liu, C. Wang, J. Ma, G. Shi, X. Yao, H. Fang, Y. Song, J. Wang, *Proc. Natl. Acad. Sci. USA* **2016**, *113*, 14739–14744; d) G. Bai, D. Gao, Z. Liu, X. Zhou, J. Wang, *Nature* **2019**, *576*, 437–441.
- [3] a) C. Morris, D. Georgakopoulos, D. Sands in *Journal de Physique IV (Proceedings)*, Vol. 121, EDP sciences, **2004**, pp. 87–103; b) E. Attard, H. Yang, A.-M. Delort, P. Amato, U. Pöschl, C. Glaux, T. Koop, C. Morris, *Atmos. Chem. Phys.* **2012**, *12*, 10667–10677.
- [4] a) A. G. Govindarajan, S. E. Lindow, *Proc. Natl. Acad. Sci. USA* **1988**, *85*, 1334–1338; b) C. P. Garnham, R. L. Campbell, V. K. Walker, P. L. Davies, *BMC Struct. Biol.* **2011**, *11*, 36; c) R. Pandey, K. Usui, R. A. Livingstone, S. A. Fischer, J. Pfaendtner, E. H. Backus, Y. Nagata, J. Fröhlich-Nowoisky, L. Schmuser, S. Mauri, J. F. Scheel, D. A. Knopf, U. Pöschl, M. Bonn, T. Weidner, *Sci Adv* **2016**, *2*, e1501630.
- [5] a) M. T. Reischel, G. Vali, *Tellus* **1975**, *27*, 414–427; b) T. Koop, B. Zobrist, *Phys. Chem. Chem. Phys.* **2009**, *11*, 10839–10850.
- [6] a) P. Jungwirth, P. S. Cremer, *Nat. Chem.* **2014**, *6*, 261–263; b) X. Chen, T. Yang, S. Kataoka, P. S. Cremer, *J. Am. Chem. Soc.* **2007**, *129*, 12272–12279; c) D. J. Tobias, J. C. Hemminger, *Science* **2008**, *319*, 1197–1198.
- [7] F. Hofmeister, *Arch. Exp. Pathol. Pharmacol.* **1888**, *24*, 247–260.
- [8] H. I. Okur, J. Hladilkova, K. B. Rembert, Y. Cho, J. Heyda, J. Dzubiella, P. S. Cremer, P. Jungwirth, *J. Phys. Chem. B* **2017**, *121*, 1997–2014.
- [9] a) K. D. Collins, M. W. Washabaugh, *Q Rev Biophys* **1985**, *18*, 323–422; b) E. E. Bruce, P. T. Bui, B. A. Rogers, P. S. Cremer, N. F. A. van der Vegt, *J. Am. Chem. Soc.* **2019**, *141*, 6609–6616.
- [10] a) H. Wex, S. Augustin-Bauditz, Y. Boose, C. Budke, J. Curtius, K. Diehl, A. Dreyer, F. Frank, S. Hartmann, N. Hiranuma, E. Jantsch, Z. A. Kanji, A. Ki-

- selev, T. Koop, O. Möhler, D. Niedermeier, B. Nillius, M. Rösch, D. Rose, C. Schmidt, I. Steinke, F. Stratmann, *Atmos. Chem. Phys.* **2015**, *15*, 1463–1485; b) C. Budke, T. Koop, *Atmos. Meas. Tech.* **2015**, *8*, 689–703; c) A. T. Kunert, M. Lamneck, F. Helleis, U. Pöschl, M. L. Pöhlker, J. Fröhlich-Nowoisky, *Atmos. Meas. Tech.* **2018**, *11*, 6327–6337.
- [11] M. A. Turner, F. Arellano, L. M. Kozloff, *J. Bacteriol.* **1990**, *172*, 2521–2526.
- [12] A. A. Zavitsas, *J. Phys. Chem. B* **2001**, *105*, 7805–7817.
- [13] K. Meister, S. Strazdaite, A. L. DeVries, S. Lotze, L. L. Olijve, I. K. Voets, H. J. Bakker, *Proc. Natl. Acad. Sci. USA* **2014**, *111*, 17732–17736.
- [14] M. Lukas, R. Schwidetzky, A. T. Kunert, U. Pöschl, J. Fröhlich-Nowoisky, M. Bonn, K. Meister, *J. Am. Chem. Soc.* **2020**, *142*, 6842–6846.
- [15] a) S. Nihonyanagi, S. Yamaguchi, T. Tahara, *J. Am. Chem. Soc.* **2014**, *136*, 6155–6158; b) X. Chen, S. C. Flores, S. M. Lim, Y. Zhang, T. Yang, J. Kherb, P. S. Cremer, *Langmuir* **2010**, *26*, 16447–16454.
- [16] A. Hudait, N. Odendahl, Y. Q. Qiu, F. Paesani, V. Molinero, *J. Am. Chem. Soc.* **2018**, *140*, 4905–4912.
- [17] F. Tang, T. Ohto, S. Sun, J. R. Rouxel, S. Imoto, E. H. G. Backus, S. Mukamel, M. Bonn, Y. Nagata, *Chem. Rev.* **2020**, *120*, 3633–3667.
- [18] K. Meister, J. G. Duman, Y. Xu, A. L. DeVries, D. M. Leitner, M. Havenith, *J. Phys. Chem. B* **2014**, *118*, 7920–7924.
- [19] M. Fitzner, G. C. Sosso, S. J. Cox, A. Michaelides, *Proc. Natl. Acad. Sci. USA* **2019**, *116*, 2009–2014.
- [20] T. F. Whale, M. A. Holden, T. W. Wilson, D. O'Sullivan, B. J. Murray, *Chem. Sci.* **2018**, *9*, 4142–4151.

Manuscript received: October 20, 2020

Accepted manuscript online: January 19, 2021

Version of record online: March 16, 2021